Title
Long-term atmospheric measurements of C1-C5 alkyl nitrates in the Pearl River Delta region of southeast China

Journal
Atmospheric Environment, 40(9)

ISSN
1352-2310

Authors
Simpson, IJ
Wang, T
Guo, H
et al.

Publication Date
2006-03-01

DOI
10.1016/j.atmosenv.2005.10.062

Available online at www.sciencedirect.com
SCIENCE DIRECT®
Atmospheric Environment 40 (2006) 1619–1632
ATMOSPHERIC ENVIRONMENT
www.elsevier.com/locate/atmosenv

Long-term atmospheric measurements of C_1–C_5 alkyl nitrates in the Pearl River Delta region of southeast China

Isobel J. Simpson[a,*], Tao Wang[b], Hai Guo[b], Y.H. Kwok[b], Frank Flocke[c], Elliot Atlas[d], Simone Meinardi[a], F. Sherwood Rowland[a], Donald R. Blake[a]

[a]*Department of Chemistry, University of California-Irvine, Irvine, CA 92697, USA*
[b]*Department of Civil and Structural Engineering, The Hong Kong Polytechnic University, Kowloon, Hong Kong*
[c]*National Center for Atmospheric Research, Boulder, CO 80307, USA*
[d]*Division of Marine and Atmospheric Chemistry, University of Miami, Miami, FL 33149, USA*

Received 11 May 2005; received in revised form 27 October 2005; accepted 27 October 2005

Abstract

Mixing ratios of seven C_1–C_5 alkyl nitrates ($RONO_2$) were measured during a 16-month study (August 2001–December 2002) at Tai O, a coastal site 30 km west of central Hong Kong in the Pearl River Delta, the fastest-growing industrial region in the world. The C_3–C_4 (rather than C_1–C_2) $RONO_2$ were most abundant throughout the study, showing the importance of photochemical (rather than marine) $RONO_2$ production in the sampled air. A lack of methyl nitrate ($MeONO_2$) enhancement during summer, when the prevailing winds are from the ocean, indicates that the South China Sea is not a region of strong $RONO_2$ emissions. By contrast, $MeONO_2$ levels during pollution episodes (up to 25 parts per trillion by volume (pptv)) were the highest that our group has recorded during urban photochemical $RONO_2$ production, as opposed to marine emissions or biomass burning. The highest summed $RONO_2$ level of the study (204 pptv) was measured in the afternoon of 7 November 2002, during an intense pollution episode that captured the highest ozone (O_3) level ever recorded in Hong Kong (203 ppbv). During pollution episodes, the average ratio of O_3 to summed $RONO_2$ was roughly 1000:1 in freshly polluted air (ethyne/CO~3–5 pptv/ppbv) and 500:1 in very freshly polluted air (ethyne/CO~6–8 pptv/ppbv). Ozone and $RONO_2$ share a common photochemical source, and their good correlation in pollution plumes shows that $RONO_2$ can be used as a tracer of photochemical O_3 production. Even $MeONO_2$ showed similar diurnal variations as the C_2–C_5 $RONO_2$, indicating a strong photochemical source despite its very slow photochemical production from methane oxidation. The decomposition of longer-chain alkoxy radicals also does not explain the high $MeONO_2$ levels, and rough calculations show that methoxy radical reaction with NO_2 appears to be a viable alternate pathway for $MeONO_2$ production in polluted atmospheres, though further measurements and modeling are required to confirm this mechanism.

Keywords: Alkyl nitrates; Photochemistry; China; Urban pollution; Ozone

1. Introduction

Alkyl nitrates ($RONO_2$) are a reservoir species for tropospheric reactive odd nitrogen (NO_y) and they

*Corresponding author. Fax: +949 824 2905.
E-mail address: isimpson@uci.edu (I.J. Simpson).

1352-2310/$ - see front matter © 2005 Elsevier Ltd. All rights reserved.
doi:10.1016/j.atmosenv.2005.10.062

share a similar photochemical formation pathway as ozone (O_3) (Flocke et al., 1998a; Talbot et al., 2000). Our understanding of the sources, distribution, and seasonal cycle of $RONO_2$ has advanced considerably over the past few years. The formation of $RONO_2$ from the oxidation of parent hydrocarbons (RH) has been known since the 1970s (Darnall et al., 1976; Atkinson et al., 1982):

$$RH + OH\cdot \rightarrow R\cdot + H_2O, \quad k_1,\ \alpha_1, \tag{1}$$

$$R\cdot + O_2 \rightarrow RO_2\cdot, \quad k_2, \tag{2}$$

$$RO_2\cdot + NO \rightarrow RO\cdot + NO_2, \quad k_3,\ 1-\alpha_2, \tag{3a}$$

$$RO_2\cdot + NO \rightarrow RONO_2, \quad k_3,\ \alpha_2, \tag{3b}$$

where k_1, k_2 and k_3 are reaction rate constants, and α_1 and α_2 are branching ratios that have recently been updated in the literature (Arey et al., 2001 and references therein). In addition to photochemical $RONO_2$ formation, the oceanic source of $RONO_2$ has been known for over a decade (Walega et al., 1992; Atlas et al., 1993; Chuck et al., 2002). Thirdly, biomass burning has recently been identified as a major point source of $RONO_2$, though these emissions are not expected to significantly impact global reactive nitrogen levels (Simpson et al., 2002).

Airborne, ground-based and ship-based studies are providing an increasingly comprehensive spatial characterization of tropospheric $RONO_2$ (e.g. Schneider et al., 1998; Blake et al., 2003a). Most recently, Blake et al. (2003a) documented changes in $RONO_2$ mixing ratios with latitude, from methyl nitrate ($MeONO_2$) and ethyl nitrate ($EtONO_2$), which are dominated by equatorial oceanic sources, through 2-propyl nitrate (2-$PrONO_2$), which has both significant oceanic and northern hemispheric (NH) sources, to 2-butyl nitrate (2-$BuONO_2$), which has mostly NH sources associated with urban/industrial hydrocarbon emissions.

The primary $RONO_2$ sinks are photolysis and reaction with the hydroxyl radical (OH):

$$RONO_2 + h\nu \rightarrow RO\cdot + NO_2, \quad J_{RONO_2}, \tag{4}$$

$$RONO_2 + OH\cdot \rightarrow \text{products}, \quad k_5, \tag{5}$$

where J_{RONO_2} and k_5 are reaction rate constants for loss by photolysis and OH, respectively. The importance of $RONO_2$ loss by photolysis decreases with increasing carbon number (Clemitshaw et al., 1997; Talukdar et al., 1997). $RONO_2$ lifetimes vary with season, latitude and altitude (Clemitshaw et al., 1997), ranging from ~1 month for $MeONO_2$ to several days for pentyl nitrates.

A winter peak and springtime decline of $RONO_2$ mixing ratios has been observed at remote sites in the high NH (e.g. Beine et al., 1996; Blake et al., 2003b). Similarly, year-round measurements at Mauna Loa (Atlas and Ridley, 1996) and Summit, Greenland (Swanson et al., 2003) show a winter maximum and summer minimum, whereas long-term $RONO_2$ measurements in Germany distinguished between a summer minimum in clean, photochemically aged air masses, vs. a summer maximum in polluted air masses (Flocke et al., 1998a). Day et al. (2003) also observed a summer maximum in air sampled downwind of Sacramento, CA.

Here, we present a 16-month record of C_1–C_5 $RONO_2$ measured at Tai O, in southeast China at the mouth of the Pearl River Delta (PRD), the fastest-growing industrial area in the world (Wang et al., 2003). The Tai O measurements are the first long-term $RONO_2$ record from Asia, and they are used to investigate the sources of $RONO_2$ sampled at Tai O; characterize seasonal pollution patterns; investigate seasonally high air pollution episodes; and investigate the relationship between ozone and summed $RONO_2$ ($\sum RONO_{2,i}$).

2. Experimental

The Tai O experimental station (22°N, 114°E, 168 m elevation) is a coastal site on the west coast of Lantau Island, about 30 km west of central Hong Kong at the mouth of the PRD where it joins the South China Sea (Fig. 1). Northeasterly winds prevail during winter, and the site is frequently impacted by urban pollution plumes originating from China, often superimposed with fresh emissions from Hong Kong. During summer, southerly winds prevail and the site receives cleaner air from the tropical Pacific Ocean and South China Sea. Local emissions from Tai O are small because of the sparse population and light traffic to the area. Major sources of traffic and power plant emissions in the region are located to the east, north, and southwest. More site details are found in Wang et al. (2003).

Between 24 August 2001 and 31 December 2002, 187 whole air samples were collected at Tai O as part of a multidisciplinary study of air quality in the Hong Kong area that also included measurements of O_3, NO_y, nitric oxide (NO), carbon monoxide

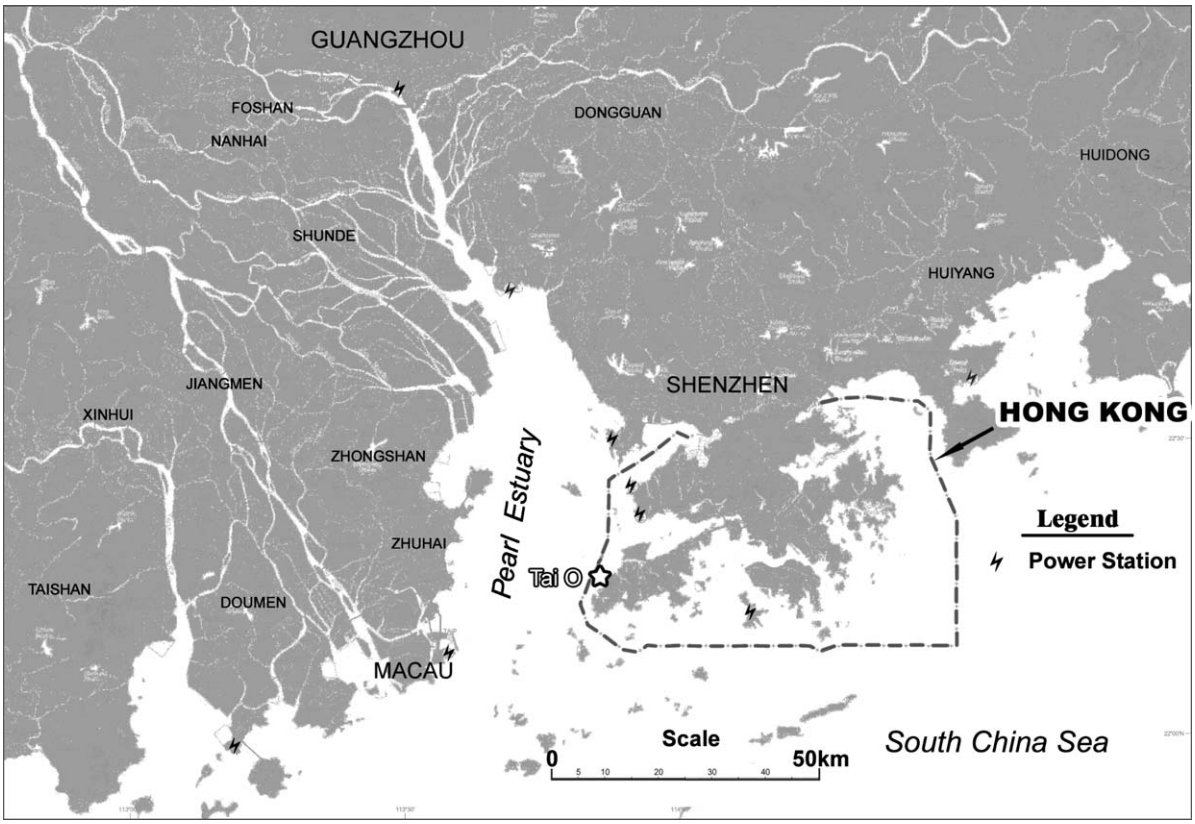

Fig. 1. Tai O sampling site in Pearl River Delta region of southeast China.

(CO), sulfur dioxide (SO_2), and meteorological parameters. Each whole air sample was collected over a 1-min period into a conditioned, evacuated 2-L stainless steel canister. Our sampling strategy emphasized pollution episodes during which samples were taken every 2 h during the daytime (between 7 a.m. and 7 p.m.). These intensive sampling periods occurred on 17–19 October 2001, 29–30 August 2002, 5–6 September 2002, 9–11 October 2002, 25 October 2002, 6–8 November 2002, and 12 November 2002. The 6–8 November episode captured the highest hourly O_3 levels ever recorded in Hong Kong (203 ppbv). Samples were taken either daily or every few days throughout the remainder of the study, typically in the mid-afternoon.

The whole air samples were analyzed for seven C_1–C_5 $RONO_2$, 42 C_2–C_{10} nonmethane hydrocarbons (NMHCs), 26 C_1–C_2 halocarbons and three sulfur compounds at the University of California, Irvine (UCI), using techniques described in Colman et al. (2001) and Simpson et al. (2003). Briefly, the $RONO_2$ were detected using gas chromatography (GC, HP-6890) with electron capture detection (ECD), and the C_2–C_{10} NMHCs were detected using GC with flame ionization detection (FID). The trace gases in each sample were preconcentrated by passing $1520 \pm 1\,cm^3$ (STP) of canister air through a stainless steel tube filled with glass beads (1/8-inch diameter) and immersed in liquid nitrogen. A mass flow controller with a maximum allowed flow of $500\,mL\,min^{-1}$ controlled the trapping process. The trace gases were revolatilized using a hot water bath and then reproducibly split into five streams. Each stream was directed to a different column–detector combination, two of which were used to analyze the $RONO_2$ (a Restek-1701 column, and a DB-5 column connected in series to a Restek-1701 column). The mixing ratios determined from both column–detector combinations were averaged to give a single mixing ratio for each sample.

A primary $RONO_2$ standard was prepared at NCAR from commercially purchased or laboratory-synthesized $RONO_2$ diluted into humidified zero air. Secondary standards of whole air were run every four samples during the analysis and were

compared to quantitative flow dilutions of the primary $RONO_2$ standard. Assignment of the $RONO_2$ mixing ratios in the primary standard was based on a combination of FID response and GC with atomic emission detection. The standard scale is currently being re-evaluated against several newly prepared $RONO_2$ mixtures. For each $RONO_2$, the mixing ratios obtained from either column showed excellent correlation ($r^2 = 0.94-0.99$). The $RONO_2$ mixing ratios obtained from the Restek-1701 column were on average 5–12% higher than those from the DB-5/Restek-1701 column, and the standard measurements were used to adjust any deviation from a 1:1 slope during the final calibration. The $RONO_2$ measurement precision is 3% for mixing ratios above 5 parts per trillion by volume (pptv) and 5% for mixing ratios below 5 pptv. The measurement accuracy is 5–10% for $MeONO_2$, $EtONO_2$ and 2-$PrONO_2$, and 10–20% for 1-propyl nitrate (1-$PrONO_2$), 2-$BuONO_2$, 2-pentyl nitrate (2-$PeONO_2$) and 3-pentyl nitrate (3-$PeONO_2$). The detection limit is 0.01 pptv.

The sampling inlets, instrumentation and calibration for O_3, NO, NO_y and CO measurements are described in Wang et al. (2003). Briefly, O_3 was measured using a commercial UV photometric instrument (Thermo-Environmental Instruments (TEI), Model 49), and NO and NO_y were detected using a modified commercial MoO/chemiluminescence analyzer (TEI, Model 42S). Data were collected every second and averaged to 1-min values. Carbon monoxide was measured with a gas filter correlation, nondispersive infrared analyzer (API, Model 300) with a heated catalytic scrubber to convert CO to carbon dioxide (CO_2) for baseline determination. The O_3 analyzer has a detection limit of 2 ppbv and a 2σ precision of 2 ppbv for a 2-min average. The NO/NO_y analyzer has a detection limit of 0.05 ppbv, a 2σ precision of 4%, and an uncertainty of about 10%.

3. Results and discussion

3.1. General features

The general features of the Tai O $RONO_2$ and their parent hydrocarbons are summarized in Table 1. Each reported $RONO_2$ was present at levels above its detection limit in every sample. As expected, minimum values were larger for the longer-lived $RONO_2$ ($MeONO_2$ and $EtONO_2$) compared to the shorter-lived species. Even though $RONO_2$ have a strong marine source, the maximum values were sampled during air pollution episodes (Section 3.2).

Table 1
Alkyl nitrate and parent hydrocarbon mixing ratio statistics (pptv) for whole air samples collected at Tai O between 24 August 2001 and 31 December 2002

Compound	Minimum	Maximum	Median	Mean	St. dev.
$MeONO_2$	2.6	24.5	6.3	7.5	4.2
$EtONO_2$	1.5	19.0	6.7	7.3	3.6
1-$PrONO_2$	0.2	11.7	2.8	3.2	2.1
2-$PrONO_2$	1.9	53.2	19.8	21.0	10.7
2-$BuONO_2$	0.7	76.8	23.4	26.3	15.4
2-$PeONO_2$	0.1	24.3	6.0	6.8	4.3
3-$PeONO_2$	0.1	19.2	5.6	6.1	3.6
Methane	1 749 000	3 702 000	1 956 000	2 052 000	299 000
Ethane	375	5 050	2 135	2 120	990
Propane	18	12 995	1 545	2 050	2 160
n-Butane	6	12 790	950	1 640	2 130
n-Pentane	5	5 595	255	450	650
NO (ppbv)	0.0	95	2	8	16
NO_y (ppbv)	1.9	160	28	36	28
O_3 (ppbv)	1.7	193	47	57	41

Mixing ratio statistics (ppbv) are also shown for nitric oxide (NO), reactive odd nitrogen (NO_y) and ozone (O_3) samples taken at the same time as the whole air samples.

The C_3–C_4 $RONO_2$ were the most abundant in the Tai O air samples (Table 1). In photochemical $RONO_2$ production, the branching ratios leading to $RONO_2$ formation increase with increasing carbon number (Atkinson et al., 1982; Arey et al., 2001), but the ambient mixing ratios of parent *n*-alkanes decrease with increasing carbon number. The net effect of these two factors is maximum photochemical production of C_3–C_4 $RONO_2$, in particular 2-$PrONO_2$ and 2-$BuONO_2$. By contrast, oceans are the dominant source of $MeONO_2$ and, to a lesser extent, $EtONO_2$ (e.g. Blake et al., 2003a). Here the relative abundance of C_3–C_4 $RONO_2$ at Tai O indicates the importance of photochemical (rather than marine) $RONO_2$ production in air masses transported to this site.

The range of $RONO_2$ mixing ratios measured at Tai O was similar to that measured by our group between 0 and 2 km in early spring 2001 during the Transport and Chemical Evolution over the Pacific (TRACE-P) field campaign, flown off the Asian coast (Simpson et al., 2003). The mean and median $RONO_2$ mixing ratios were 1.6–2.1 times higher at Tai O than during TRACE-P, which is not unexpected given the closer proximity to urban

sources at Tai O and a bias towards sampling during pollution episodes. The similar maximum and minimum values at Tai O and during TRACE-P suggest that both field studies captured the full range of $RONO_2$ mixing ratios that are typical along the southeast Asian coast.

3.2. Seasonal pattern

The $RONO_2$ measured at Tai O show a winter maximum and summer minimum (Fig. 2). This pattern is opposite to that observed for polluted air masses at temperate sites in North America and Europe, and happens to match the $RONO_2$ seasonality that has been observed in photochemically aged air (Section 1). At the subtropical Tai O site, the $RONO_2$ seasonality is explained by the seasonal wind pattern, which brings polluted air from the east and north in winter, and cleaner marine air from the south in summer (Section 2). Also due to local wind patterns, Flocke et al. (1998a) observed a summer maximum in polluted air masses in Germany, which were transported to the sampling site more frequently during summer than in winter. The seasonal pattern for the $RONO_2$ is similar to that for other trace gases measured at the Tai O site such as CO, NMHCs, NO_y and SO_2 (Wang et al., 2005).

The seasonal $RONO_2$ pattern at Tai O shows considerable day-to-day variability depending on the intensity of pollution episodes (Fig. 2). The magnitudes of the summer minima at Tai O are similar to those measured at the remote Summit, Greenland site, ranging from 1 to 2 pptv and 0.5 to 1 pptv for 2-$PrONO_2$ and 2-$BuONO_2$, respectively (Table 1; Swanson et al., 2003). These low values reflect the clean marine air sampled at Tai O during summer. The maximum $RONO_2$ mixing ratios at Tai O are within the range of maxima that have been measured at other urban sites. The respective peak 2-$PrONO_2$ and 2-$BuONO_2$ mixing ratios at Tai O were 53 and 77 pptv, compared to 34 and 45 pptv in urban samples collected in Karachi, Pakistan during winter (Barletta et al., 2002), and 67 and 79 pptv in fresh Asian outflow measured downwind of Shanghai during the springtime TRACE-P mission (Simpson et al., 2003). Flocke et al. (1998a) measured a higher 2-$PrONO_2$ maximum of 79 pptv downwind of Freiburg and the Rhine Valley, Germany during summer.

Interestingly $MeONO_2$ shows the same seasonal pattern as the higher $RONO_2$, despite the much slower reaction of its parent hydrocarbon methane (CH_4) with OH, compared to parent *n*-alkanes $\geqslant C_2$. The photochemical production of $MeONO_2$ at this site is discussed in Section 3.3.2. Blake et al. (2003a) observed high $MeONO_2$ mixing ratios (up to 50 pptv) in the equatorial Pacific as a result of marine emissions, and lower values (<6 pptv) to the north of the equatorial enhancements. At Tai O, the lack of $MeONO_2$ enhancements during the summer (median = 5 pptv between April and August 2002) indicates that the marine air transported to this site was not strongly influenced by oceanic $MeONO_2$ emissions. Consistent with this, Blake et al. (2003a) found that in the Pacific south of 10°N, marine $RONO_2$ were emitted in the following ratios: $MeONO_2$/$EtONO_2$, 3:1; $MeONO_2$/2-$PrONO_2$, 10:1; $MeONO_2$/2-$BuONO_2$, 50:1. Here, the average ratios for the summer samples were $MeONO_2$/$EtONO_2$, 2:1; $MeONO_2$/2-$PrONO_2$, 1:1; $MeONO_2$/2-$BuONO_2$, 2:1. These much lower Tai O ratios are typical of NH air masses influenced by urban/industrial emissions (Blake et al., 2003a) and they confirm a lack of strong marine $RONO_2$ emissions in the Tai O samples.

The C_1–C_5 $RONO_2$ measured at Tai O comprise a small fraction of NO_y (0.3–8% during winter and 1–6% during summer; see Table 1). $RONO_2$ typically comprise less than 10% of NO_y in continental air masses (e.g. Buhr et al., 1990; Shepson et al., 1993; Talbot et al., 2003)—with reports of 10–20% of NO_y using a more broad definition of total $RONO_2$ (Day et al., 2003)—compared to 20–80% in the equatorial marine boundary layer over the Pacific (Talbot et al., 2000; Blake et al., 2003a). At Tai O the low $RONO_2$ fraction is explained by the wintertime sampling of polluted continental air masses, and the summertime sampling of oceanic air that was not strongly influenced by marine $RONO_2$ sources.

3.3. Pollution episodes

3.3.1. Maximum O_3 and $RONO_2$ mixing ratios

The strongest pollution episode of the 16-month study was sampled from 6 to 8 November 2002, with very high levels of parent *n*-alkanes and high rates of daughter $RONO_2$ production, especially on 7 November (Fig. 3). The prevailing winds on 7 November were from the east and northeast, and a cold front pushed continental air to the Tai O site. The ratio of ethyne/CO reflects the amount of atmospheric processing (photochemical reaction

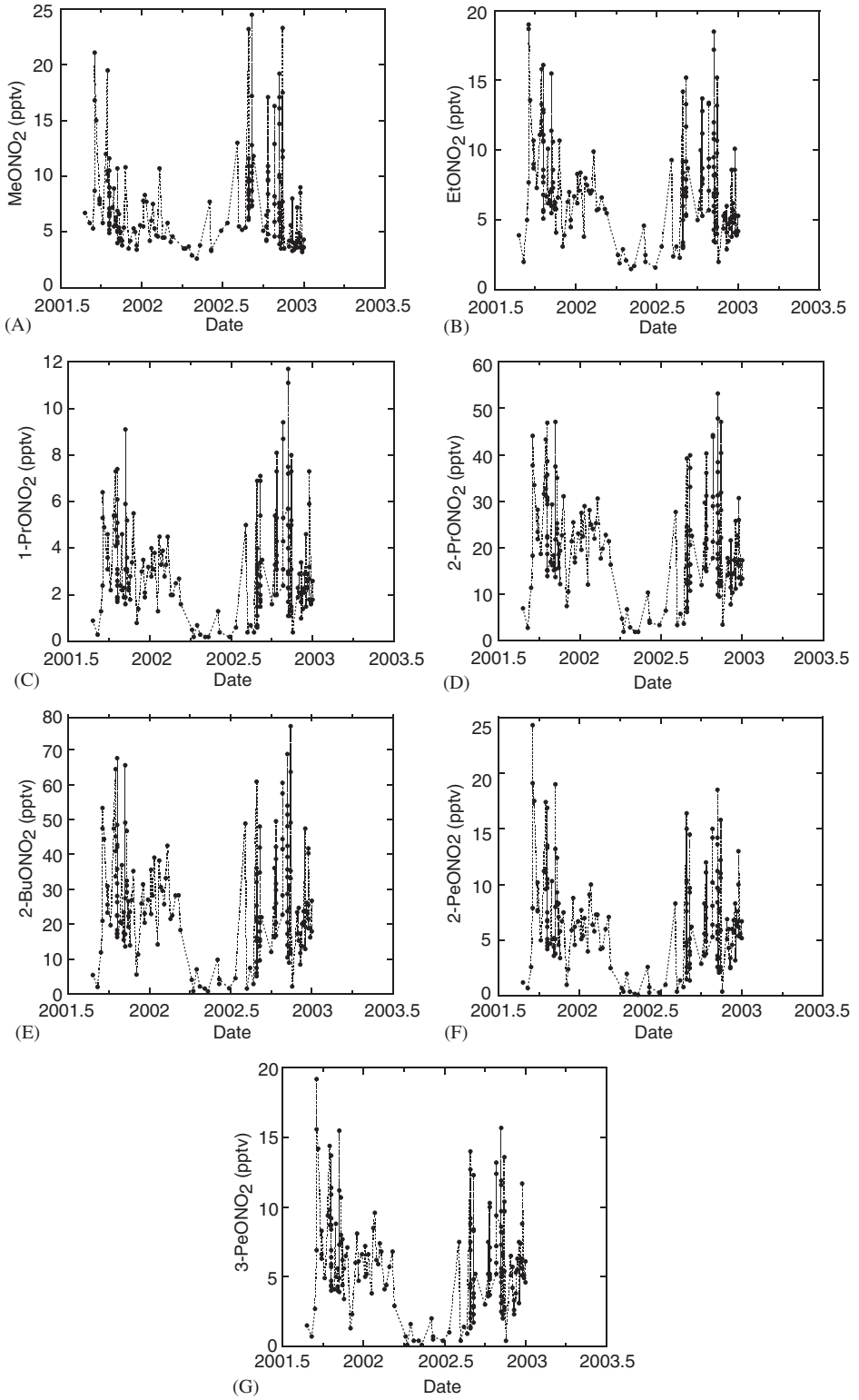

Fig. 2. Alkyl nitrate mixing ratios (pptv) measured at Tai O between August 2001 and December 2002: (A) methyl nitrate; (B) ethyl nitrate; (C) 1-propyl nitrate; (D) 2-propyl nitrate; (E) 2-butyl nitrate; (F) 2-pentyl nitrate; and (G) 3-pentyl nitrate.

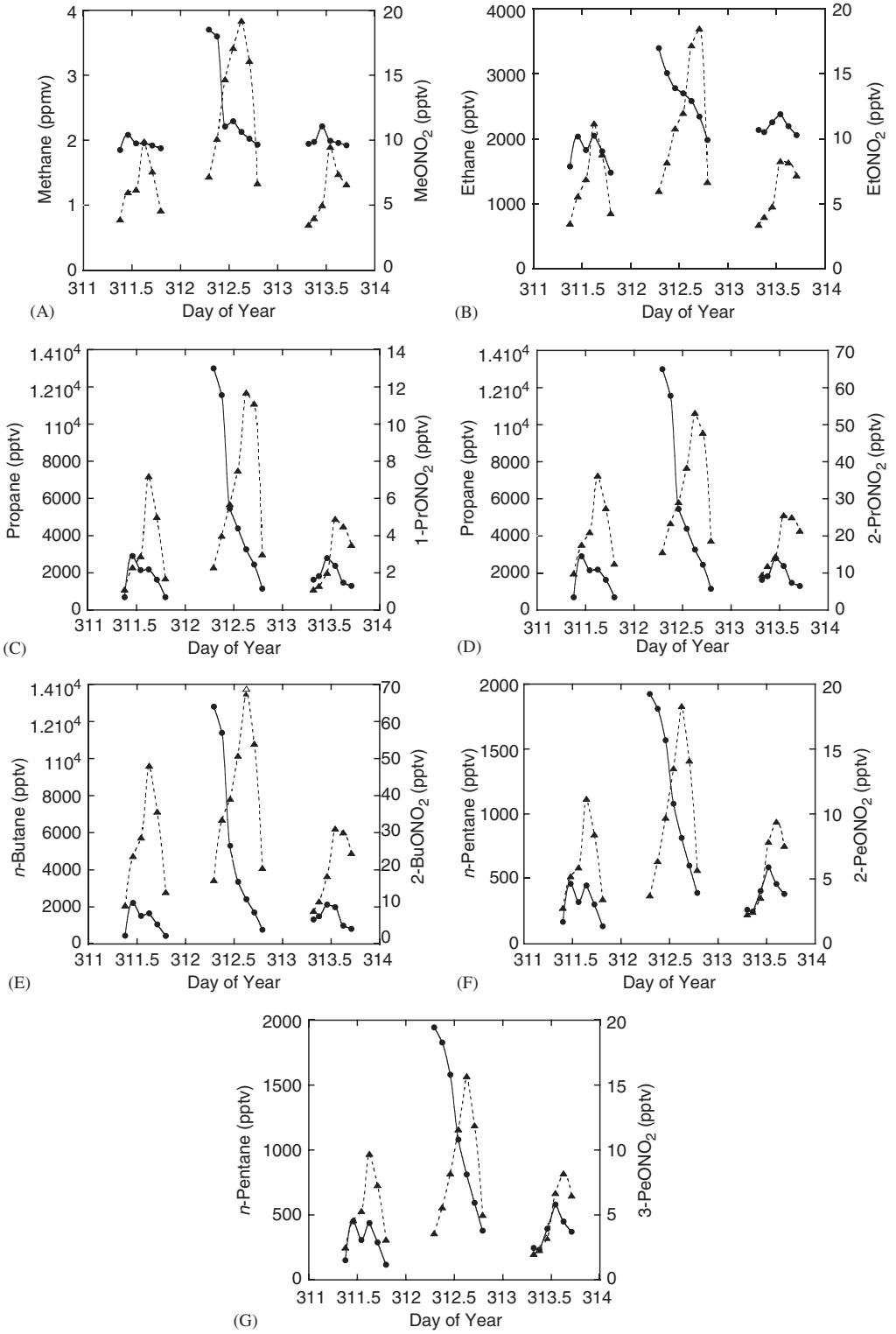

Fig. 3. Parent *n*-alkane mixing ratios (circles and solid line) and daughter alkyl nitrate mixing ratios (triangles and dashed line) measured during pollution episode of 6–8 November 2002: (A) methane and methyl nitrate; (B) ethane and ethyl nitrate; (C) propane and 1-propyl nitrate; (D) propane and 2-propyl nitrate; (E) *n*-butane and 2-butyl nitrate; (F) *n*-pentane and 2-pentyl nitrate; and (G) *n*-pentane and 3-pentyl nitrate.

and dynamic mixing) within an air mass (Smyth et al., 1996), decreasing from 4 to 5 pptv/ppbv for freshly polluted air to <1 pptv/ppbv for very processed air (E. Browell, pers. comm., 2002). On 7 November the ethyne/CO ratio decreased from 11.4 pptv/ppbv at 7 a.m. to 2.8 pptv/ppbv at 7 p.m., indicating that the air masses sampled early in the morning were very freshly polluted, whereas those sampled later in the day were increasingly processed.

The highest hourly O_3 level ever recorded in Hong Kong (203 ppbv) was measured during this pollution episode, on 7 November at 4 p.m. The highest 1-$PrONO_2$ and 2-$PrONO_2$ mixing ratios of the study (12 and 53 pptv, respectively; Table 1) were also measured on 7 November, at 3 p.m. The mixing ratios of $MeONO_2$, $EtONO_2$, 2-$BuONO_2$, 2-$PeONO_2$ and 3-$PeONO_2$ (19, 17, 69, 19 and 16 pptv, respectively) were also strongly elevated in this sample. Whole air samples were collected every 2 h during pollution episodes, whereas O_3 was averaged every minute (Section 2). Therefore, it is possible that the actual $RONO_2$ maxima occurred closer to 4 p.m. rather than 3 p.m. On the other hand, during a summertime study in Texas, Rosen et al. (2004) observed that the daily total $RONO_2$ maximum occurred earlier in the afternoon than the O_3 maximum.

Propane mixing ratios were 13.0 ppbv at 7 a.m. on 7 November, and decreased throughout the day to 1.2 ppbv by 7 p.m. (Fig. 3C). By comparison, propane mixing ratios over the western Pacific typically range from 0.5 to 2 ppbv at latitudes comparable to Tai O (Blake et al., 1997). The measured *n*-butane levels decreased by 94% during the same 12-h period, from 12.8 to 0.8 ppbv (Fig. 3E), and the measured *n*-pentane levels decreased by 80%, from 1.9 to 0.4 ppbv (Fig. 3F). Daughter $RONO_2$ are photochemically produced as the parent *n*-alkane is oxidized (Eqs. (1)–(3)). On 7 November, the 2-$PrONO_2$, 2-$BuONO_2$ and 2-$PeONO_2$ mixing ratios increased at respective average rates of about 4.7, 6.5 and 1.9 pptv h^{-1} between 7 a.m. and 3 p.m., with maximum increases of 6.0, 7.5 and 2.2 pptv h^{-1} between 11 a.m. and 3 p.m. Very strong O_3 increases also occurred on 7 November, at an average rate of 25 ppbv h^{-1} between 7 a.m. and 3 p.m., and 45 ppbv h^{-1} between 11 a.m. and 3 p.m.

The measured *n*-alkane decreases on 7 November are much larger than can be accounted for by OH-chemistry alone, which was roughly predicted for the air mass sampled at 7 a.m. using:

$$[RH] = [RH]_0 \, e^{-k_A t}, \quad (6)$$

where t is the elapsed time between parent *n*-alkane emission and air sampling, and k_A is $k_1[OH]$ (Table 2). Although we could not follow this air mass for a Lagrangian analysis, we perform this calculation to test what alkane changes we might have expected for this air mass due to OH oxidation, and whether or not these changes are similar to those observed for upwind air masses that were sampled throughout the day on 7 November. Hydroxyl radicals show a strong diurnal variation (Kramp and Volz–Thomas, 1997; Hofzumahaus et al., 1998), and a daytime OH value of 4×10^6 molec cm^{-3} was used to compare the predicted *n*-alkane depletion with that measured on 7 November. After 12 h of photochemical processing, *n*-butane is predicted to have become depleted by about 35%, from 12.8 ppbv at 7 a.m. to 8.4 ppbv at 7 p.m. (not shown). Shorter-lived *n*-pentane is expected to decrease by about 50% under the same conditions, from 1.9 to 1.0 ppbv (not shown). These predicted *n*-alkane decreases are much smaller than the large decreases that were measured on 7 November. Therefore, the strong *n*-butane and *n*-pentane decreases on 7 November are explained by the sampling of less polluted air masses that were transported to the site throughout the day. These results illustrate the complex mixture of very freshly polluted and processed pollution plumes that occur in the PRD. Such rapid changes in air-mass chemical characteristics have also been shown from an analysis of continuously measured O_3, CO, SO_2 and NO_y at the Tai O site (Wang and Kwok, 2003; Wang et al., 2003).

Table 2
Kinetic data and branching ratios for the C_4–C_5 alkyl nitrates measured at Tai O

Compound	k_1[a]	k_4[b]	α_1[c]	α_2[d]	J[e]
2-$BuONO_2$	2.44	0.92	0.872	0.084	0.47
2-$PeONO_2$	4.0	1.85	0.568	0.106	0.46
3-$PeONO_2$	4.0	1.12	0.349	0.126	0.44

Units for k: $\times 10^{-12}$ cm^3 $molec^{-1}$ s^{-1}; for J: $\times 10^{-6}$ s^{-1}.
[a]Atkinson (1997).
[b]Atkinson (1990), Atkinson et al. (1997).
[c]Kwok and Atkinson (1995).
[d]Atkinson et al. (1995), Arey et al. (2001).
[e]1 April, 40°N, diurnal J-value.

3.3.2. Photochemical $MeONO_2$ production

In addition to a similar seasonal pattern as the higher $RONO_2$ (Section 3.2), $MeONO_2$ also displayed a similar diurnal pattern. For example, during the 6–8 November pollution episode its daily variations were almost identical to those of the C_2–C_5 $RONO_2$ (Fig. 3). The highest $MeONO_2$ mixing ratio of the study (24.5 pptv) was measured at 11 a.m. on 6 September 2002 (Table 1). By comparison, Barletta et al. (2002) measured a much lower $MeONO_2$ maximum of 13.3 pptv in urban Karachi, Stroud et al. (2001) measured a $MeONO_2$ maximum of 6.5 pptv over rural Colorado, and Roberts et al. (1998) measured a maximum of 3.5 pptv in Nova Scotia. Global background $MeONO_2$ mixing ratios vary little with latitude in the Northern Hemisphere, and year-round values range from about 3 to 5 pptv (Blake, 2004). Therefore, of the 24.5 pptv $MeONO_2$ measured on 6 September, about 20 pptv is in excess of background values.

Although our group has measured larger $MeONO_2$ mixing ratios in samples influenced by biomass burning or marine $RONO_2$ sources (Simpson et al., 2002; Blake et al., 2003a), the $MeONO_2$ levels at Tai O are the largest that we have measured in urban pollution plumes. Despite very high CH_4 levels measured on 6 September at 11 a.m. (3.28 ppmv), CH_4 oxidation accounts for only a small fraction of the $MeONO_2$ produced in this air mass. Methane is very long-lived (~8 years; Lelieveld et al., 1998; Karlsdóttir and Isaksen, 2000) compared to the C_2–C_5 alkanes (days–months), and the photochemical production of its daughter $RONO_2$ is limited in part by the slow production of $CH_3^{\bullet}$ during CH_4 oxidation:

$$CH_4 + OH\cdot \rightarrow CH_3\cdot + H_2O, \quad k_7,\ \alpha_7, \qquad (7)$$

where $k_7 = 6.18 \times 10^{-15}\,cm^3\,molec^{-1}\,s^{-1}$ at 298 K (Atkinson, 1997) and $\alpha_7 = 1$ (Kwok and Atkinson, 1995). Applying Eq. (6) using $[CH_4]_0 = 3\,280\,000$ pptv, $t = 24$ h and assuming a diurnal OH value of $2 \times 10^6\,molec\,cm^{-3}$ gives CH_4 loss of about 3500 pptv after 1 day of photochemical processing. (Ethyne/CO was 5.4 pptv/ppbv in the 11 a.m. air mass—indicating freshly polluted air—and therefore 3.28 ppmv is a good approximation of $[CH_4]_0$.) The reaction described by Eq. (2) is fast and the 3500 pptv of CH_3 radicals will be quickly converted to 3500 pptv of CH_3O_2 radicals. For tropospheric conditions, Flocke et al. (1998b) estimate an upper limit of 0.0003 for the branching ratio α_2 that leads to $MeONO_2$ formation. Therefore, 3500 pptv of CH_3O_2 radicals are expected to give rise to no more than about 1 pptv of $MeONO_2$ in 1 day and 7 pptv in 7 days (of which some will be consumed by photolysis). As a result, most of the 20 pptv of excess $MeONO_2$ measured in this pollution plume was formed via alternative photochemistry. A similar calculation for $EtONO_2$ shows that ethane oxidation is not sufficient to explain the 13 pptv of $EtONO_2$ that was measured (ethane oxidation yields roughly 4 pptv of $EtONO_2$ after 1 day and 8 pptv after 7 days). In their German study, Flocke et al. (1998a) also observed higher levels of $MeONO_2$ and $EtONO_2$ than could be explained by Eq. (3b).

For $RONO_2 \leqslant C_4$, oxidation of the parent hydrocarbon is not the only source of daughter RO_2 radicals, and instead a significant RO_2 fraction is formed from the decomposition of larger alkoxy radicals (Bertman et al., 1995; Flocke et al., 1998a). However, at Tai O this mechanism is insufficient for $MeONO_2$ because of the extremely small α_2 branching ratio for $MeONO_2$ formation (0.0003), which requires the mixing ratio of CH_3O_2 radicals to be unreasonably large. A possible alternate pathway for the excess $MeONO_2$ formation is via:

$$CH_3O\cdot + NO_2 + M \rightarrow CH_3ONO_2 + M, \quad k_8, \qquad (8)$$

where $k_8 = 1.6 \times 10^{-11}\,cm^3\,molec^{-1}\,s^{-1}$ at 298 K (DeMore et al., 1997). This mechanism is independent of the very small $CH_4 + OH$ rate constant and very small $CH_3O_2 + NO$ branching ratio. Although Eq. (8) is a minor $RONO_2$ formation pathway under normal conditions, Flocke et al. (1998a, b) postulated that a possible exception may be the formation of $MeONO_2$ under very polluted conditions. Because the excess $MeONO_2$ at Tai O is not explained by marine emissions, CH_4 oxidation or the decomposition of larger alkoxy radicals, reaction of the methoxy radical with NO_2 appears to be the most likely source of $MeONO_2$ in the heavily polluted plumes that were sampled at Tai O. This pathway requires significant amounts of NO_2 because of the competing reaction of CH_3O with O_2 to form formaldehyde (HCHO):

$$CH_3O\cdot + O_2 \rightarrow HCHO + HO_2\cdot, \quad k_9, \qquad (9)$$

where $k_9 = 1.9 \times 10^{-15}\,cm^3\,molec^{-1}\,s^{-1}$ at 298 K (DeMore et al., 1997). Because the CH_3O required for $MeONO_2$ formation also yields HCHO, additional data on chemical composition and conditions at the source, as well as chemical box modeling, are required in order to fully verify whether this

proposed mechanism for $MeONO_2$ formation is sufficient and compatible with other measurements (such as HCHO). Below we perform a rough calculation (which does not account for diurnal variations of temperature, mixing ratio, etc.) to determine whether or not this mechanism is "in the right ballpark" for producing sufficient quantities of $MeONO_2$.

We have assumed $CH_3O_2 + NO \rightarrow CH_3O + NO_2$ (Eq. (3a), $k = 7.56 \times 10^{-12}\,cm^3\,molec^{-1}\,s^{-1}$ at 30 °C) as the predominant source of CH_3O radicals; an urban CH_3O_2 mixing ratio of 5 pptv ($1.2 \times 10^8\,molec\,cm^{-3}$); and a measured NO mixing ratio of 8 ppbv ($2.0 \times 10^{11}\,molec\,cm^{-3}$) on 6 September at 11 a.m. to give a rough CH_3O production rate of 7 pptv s^{-1} ($1.8 \times 10^8\,molec\,cm^{-3}\,s^{-1}$). The branching ratio for the reactions of CH_3O described by Eqs. (8) and (9) is given by

$$(k_8 \times [NO_2])/(k_9 \times [O_2]). \quad (10)$$

In urban areas where NO sources are large, NO_2 and NO typically comprise a major fraction of NO_y (Seinfeld and Pandis, 1998 and references therein). At 11 a.m. on 6 September we measured $NO_y =$ 104 ppbv, and here we use an NO_2 test value of 50 ppbv, or 5×10^{-8} parts per part by volume. The atmosphere is comprised of about 21% O_2 by volume, or 0.21 parts per part by volume. Solving Eq. (10) under these conditions gives a branching ratio of 0.000084, which when multiplied by the CH_3O production rate of 7 pptv s^{-1} gives a $MeONO_2$ production rate of 0.00059 pptv s^{-1}, or 50 pptv day^{-1}. This is of the right order of magnitude to explain the 20 pptv of excess $MeONO_2$ that was observed during this study. A lower $MeONO_2$ production rate would be achieved with a lower NO_2 or RO_2 mixing ratio, and a higher production rate with a higher NO_2 or RO_2 mixing ratio. These rough calculations show that photochemical CH_3ONO_2 production via $CH_3O + NO_2$ reaction appears to be likely in polluted cities, though we suggest more comprehensive modeling in order to confirm this mechanism.

Another possible mechanism for $MeONO_2$ formation in cities is the liquid phase acid-catalyzed reaction of methanol (CH_3OH) with nitric acid (HNO_3) (L. Iraci, pers. comm., 2005). This newly considered aerosol mechanism is under continued investigation to determine whether or not it is plausible for acidities that are typical in a city.

3.3.3. $RONO_2$ relationships with O_3

Reactions (1–3), which form $RONO_2$, also produce NO_2 and lead to tropospheric O_3 formation:

$$NO_2 + h\nu \rightarrow NO + O, \quad (11)$$

$$O + O_2 + M \rightarrow O_3 + M. \quad (12)$$

During the seven intensive pollution episodes sampled at Tai O (Section 2, $n = 79$), the median O_3 mixing ratio was 66 ppbv; the median summed $RONO_2$ mixing ratio ($\sum RONO_{2,i} = MeONO_2 + EtONO_2 + 1\text{-}PrONO_2 + 2\text{-}PrONO_2 + 2\text{-}BuONO_2 + 2\text{-}PeONO_2 + 3\text{-}PeONO_2$) was 78 pptv, and the median ratio of $O_3/\sum RONO_{2,i}$ was 830 pptv/pptv. Similarly, the average mixing ratio (± 1 standard error) was 69 ± 8 ppbv for O_3 and 89 ± 10 pptv for $\sum RONO_{2,i}$, and their average ratio was 810 pptv/pptv. A plot of O_3 vs. $\sum RONO_{2,i}$ during these pollution episodes shows considerable scatter ($r^2 = 0.46$, though this improves when the seven episodes are considered separately) and, for a linear fit, gives a slope of 655 pptv/pptv and an intercept of about 11 ppbv O_3 for zero $RONO_{2,i}$ (Fig. 4A).

During the seven pollution episodes, the O_3 and $\sum RONO_{2,i}$ mixing ratios were lowest in the morning and peaked in the mid-afternoon (e.g. Fig. 5), as expected in response to daytime photochemistry and despite the expansion of the daytime boundary layer. The $O_3/\sum RONO_{2,i}$ ratio increased during the day, with a wide range of morning values (95–845 pptv/pptv at 9 a.m.) depending largely on variations in O_3 levels. By 3 p.m., when O_3 and $RONO_2$ values approached their daily maxima, $O_3/\sum RONO_{2,i}$ ranged from 520 to 1550 pptv/pptv. During these pollution episodes the mean $O_3/\sum RONO_{2,i}$ ratio (± 1 standard error) was 440 ± 50 pptv/pptv at 9 a.m., and 1030 ± 115 pptv/pptv at 3 p.m. Consistent with our results, $O_3/\sum RONO_{2,i}$ vs. ethyne/CO shows considerable scatter but an overall negative relationship (Fig. 4B). (From Section 3.3.2, the ratio of ethyne/CO decreases as an air mass becomes increasingly photochemically processed.) Using thermal dissociation-laser-induced fluorescence (TD-LIF), Rosen et al. (2004) also observed an increasing slope for O_3 vs. total $RONO_2$ from morning to afternoon. However, because the TD-LIF measurements include other $RONO_2$ species not measured in our canisters (i.e. total $RONO_2 > \sum RONO_{2,i}$), they observed a smaller $O_3/RONO_2$ ratio. Bearing in mind the scatter in our data, these results suggest a

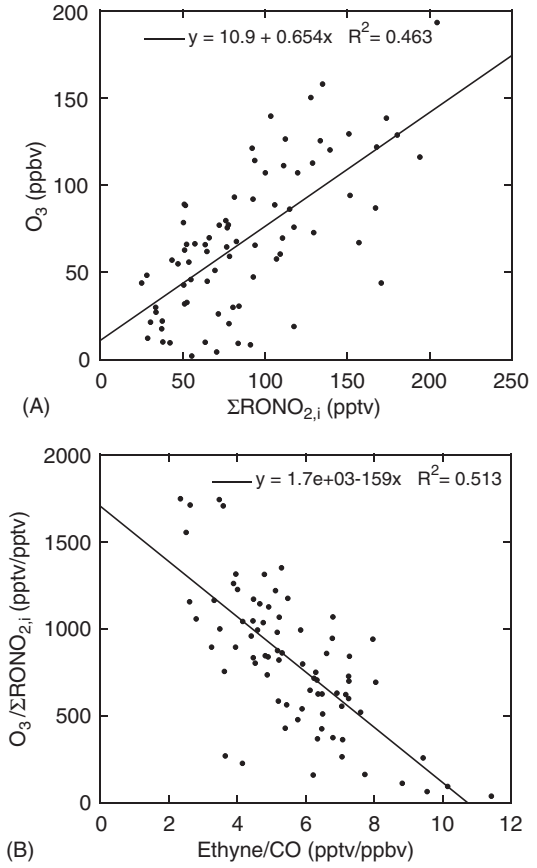

Fig. 4. (A) Ozone vs. summed alkyl nitrate ($\sum RONO_{2,i}$) mixing ratios and (B) ozone/$\sum RONO_{2,i}$ vs. ethyne/CO measured during seven intensively sampled pollution episodes at Tai O ($n = 79$; see Section 2 for sampling dates).

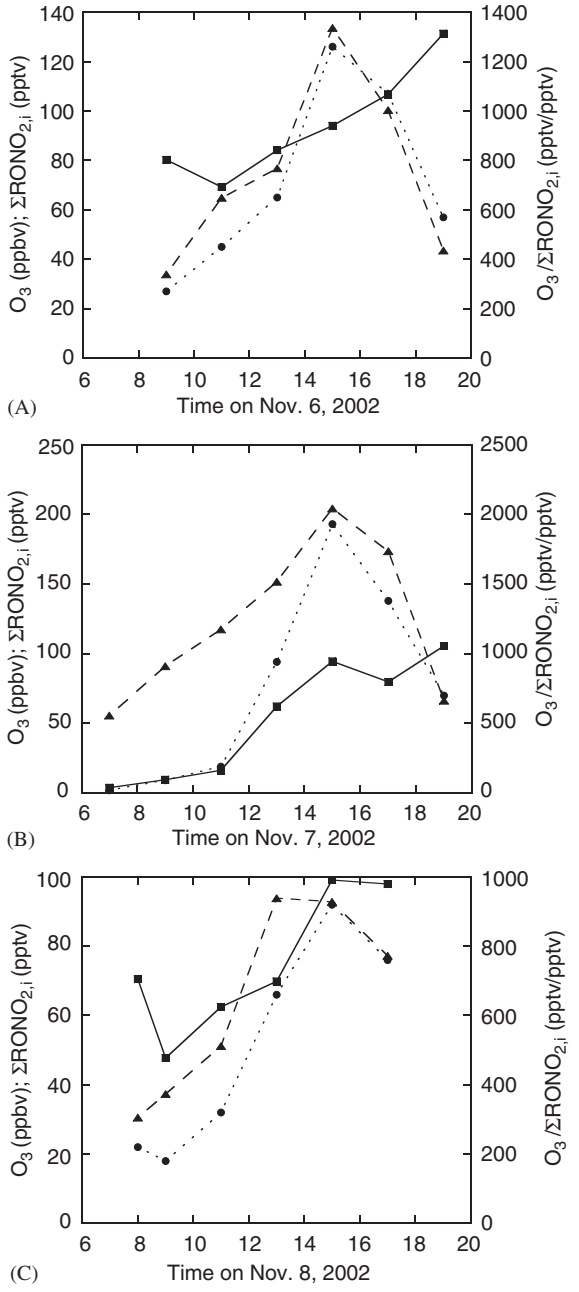

Fig. 5. Summed alkyl nitrate ($\sum RONO_{2,i}$) mixing ratios (triangles and dashed line), ozone mixing ratios (circles and dotted line), and ratio of ozone/$\sum RONO_2$ (squares and solid line): (A) 6 November 2002; (B) 7 November 2002; and (C) 8 November 2002.

rough $O_3/\sum RONO_{2,i}$ ratio of 500:1 in very freshly polluted plumes (ethyne/CO~6–8 pptv/ppbv), and a higher $O_3/\sum RONO_{2,i}$ ratio on the order of 1000:1 in freshly polluted plumes (ethyne/CO~3–5 pptv/ppbv). Though the $O_3/\sum RONO_{2,i}$ ratios show a large range, the similar diurnal variations of O_3 and $RONO_2$ during pollution episodes show that $RONO_2$ can be used as indicators of photochemical O_3 production.

The $O_3/\sum RONO_{2,i}$ relationships measured at Tai O were compared with those measured during an encounter with a fresh, well-defined pollution plume over the East China Sea at an altitude of 330 m during the springtime TRACE-P mission. Backward trajectories showed that the air mass had encountered Shanghai 18 h prior to sampling, and a high ethyne/CO ratio (5.0–9.4 pptv/ppbv) confirmed that the plume had been very recently polluted (Simpson et al., 2003). A plot of O_3 vs. $\sum RONO_{2,i}$ showed excellent correlation ($r^2 = 0.96$; $n = 7$) with a slope of 496 pptv/pptv and an intercept of 25 ppbv O_3 for zero $RONO_2$. This slope agrees remarkably well with that measured in the most freshly polluted plumes at Tai O (ethyne/CO~6–8 pptv/ppbv). That

is, the O_3 vs. $\sum RONO_{2,i}$ relationship shows robustness for young air masses collected in a similar region during different seasons. Rosen et al. (2004) also found remarkably similar agreement for O_x ($=O_3+NO_2$) vs. $\sum RONO_{2,i}$ measured in Texas and in Germany (Flocke et al., 1998a). By contrast, we expect a poorer agreement in other instances. For example, at Tai O there were several cases of high $\sum RONO_{2,i}$ at low O_3 (Fig. 4A), which we believe is due to titration of O_3 by NO:

$$O_3 + NO \rightarrow O_2 + NO_2. \quad (13)$$

In other environments, O_3 formation from biogenic hydrocarbon emissions (e.g. isoprene) is expected to greatly affect the measured O_3 vs. total $RONO_2$ ratios (Day et al., 2003). Therefore, despite the good agreement between Tai O and TRACE-P, we do not suggest applying the $O_3/\sum RONO_{2,i}$ relationships measured at Tai O quantitatively to other studies before preliminary O_3 vs. $\sum RONO_{2,i}$ comparisons are made.

4. Conclusions

Mixing ratios of seven C_1–C_5 $RONO_2$ were recorded during a 16-month study (August 2001–December 2002) at Tai O, a coastal site in southeast China located about 30 km west of central Hong Kong. Prevailing northeasterly winds during autumn and winter often brought polluted continental air from Hong Kong and mainland China to the site, whereas prevailing southerly winds during spring and summer transported cleaner marine air to Tai O. Photochemical (rather than marine) production is the dominant $RONO_2$ source at this site.

$MeONO_2$ is a tracer of marine $RONO_2$ production, and a lack of $MeONO_2$ enhancement during summer indicates that the South China Sea is not a region of strong $RONO_2$ emission. Interestingly, $MeONO_2$ showed a similar diurnal and seasonal pattern to the higher $RONO_2$. $MeONO_2$ levels during pollution episodes reached 25 pptv and were the highest we have measured during urban photochemical $RONO_2$ production. Marine emissions, methane oxidation and the decomposition of longer-chain alkoxy radicals do not fully account for the high $MeONO_2$ levels. Rough calculations, which require confirmation from modeling studies, show that methoxy radical reaction with NO_2 appears to be a viable alternate pathway for $MeONO_2$ production in polluted atmospheres.

The strongest pollution episode of the study was measured on 7 November 2002, during which ozone reached the highest level ever recorded in Hong Kong (203 ppbv). The maximum 2-$PrONO_2$ and 2-$BuONO_2$ mixing ratios on 7 November were 53 and 69 pptv, respectively, and the 2-$PrONO_2$ and 2-$BuONO_2$ levels increased by 6 and 7.5 pptv h^{-1}, respectively, between 11 a.m. and 3 p.m. Ozone and summed $RONO_2$ showed similar diurnal variations during pollution episodes, indicating that $RONO_2$ can be used as tracers of photochemical O_3 production from anthropogenic precursors. We observed an $O_3/\sum RONO_{2,i}$ ratio on the order of 500:1 in very freshly polluted air (ethyne/CO~6–8 pptv/ppbv) and 1000:1 in freshly polluted air (ethyne/CO~3–5 pptv/ppbv). However, we do not recommend applying these relationships quantitatively elsewhere, in cases where either O_3 or $RONO_2$ measurements are not available, without a better understanding of how $O_3/\sum RONO_{2,i}$ varies in different environments.

Acknowledgments

We are grateful to Dr. Vincent Cheung and Mr. Steven Poon for their help with the Tai O field measurements. This research was funded by the Research Grants Council of the Hong Kong SAR (Project PolyU5059/00E), with additional financial support provided by the Hong Kong Polytechnic University. We thank the UCI team for laboratory analysis of the whole air samples, especially Mr. Rafe Day, Mr. Kevin Gervais and Mr. Brent Love. Ozone data from TRACE-P are courtesy of Dr. Melody Avery (NASA-Langley). We also thank numerous colleagues for their valuable insights into possible mechanisms for photochemical $MeONO_2$ formation, especially Dr. Laura Iraci for sharing unpublished data with us. In addition, we thank two reviewers for their constructive comments on the manuscript.

References

Arey, J., Aschmann, S.M., Kwok, E.S.C., Atkinson, R., 2001. Alkyl nitrate, hydroxyalkyl nitrate, and hydroxycarbonyl formation from the NO_x-air photooxidations of C_5–C_8 *n*-alkanes. Journal of Physical Chemistry 105, 1020–1027.

Atkinson, R., 1990. Gas-phase tropospheric chemistry of organic compounds: a review. Atmospheric Environment 24, 1–41.

Atkinson, R., 1997. Gas-phase tropospheric chemistry of volatile organic compounds: 1. Alkanes and alkenes. Journal of Physical and Chemical Reference Data 26, 215–290.

Atkinson, R., Aschmann, S.M., Carter, W.P.L., Winer, A.M., Pitts Jr., J.N., 1982. Alkyl nitrate formation from the NO_x-air photooxidations of C_2–C_8 *n*-alkanes. Journal of Physical Chemistry 86, 4563–4569.

Atkinson, R., Kwok, E.S.C., Arey, J., Aschmann, S.M., 1995. Reactions of alkoxyl radicals in the atmosphere. Faraday Discussions 100, 23–27.

Atkinson, R., Baulch, D.L., Cox, R.A., Hampson Jr., R.F., Kerr, J.A., Rossi, M.J., Troe, J., 1997. Evaluated kinetic, photochemical and heterogeneous data for atmospheric chemistry: Supplement V. IUPAC subcommittee on gas kinetic data evaluation for atmospheric chemistry. Journal of Physical and Chemical Reference Data 26, 521–1011.

Atlas, E., Pollock, W., Greenberg, J., Heidt, L., Thompson, A.M., 1993. Alkyl nitrates, nonmethane hydrocarbons, and halocarbon gases over the equatorial Pacific Ocean during SAGA 3. Journal of Geophysical Research 98, 16,933–16,949.

Atlas, E.L., Ridley, B.A., 1996. The Mauna Loa Observatory Photochemistry Experiment: introduction. Journal of Geophysical Research 101 (D9), 14,531–14,541.

Barletta, B., Meinardi, S., Simpson, I.J., Khwaja, H.A., Blake, D.R., Rowland, F.S., 2002. Mixing ratios of volatile organic compounds (VOCs) in the atmosphere of Karachi, Pakistan. Atmospheric Environment 36 (N21), 3429–3443.

Beine, H.J., Jaffe, D.A., Blake, D.R., Atlas, E., Harris, J., 1996. Measurements of PAN, alkyl nitrates, ozone, and hydrocarbons during spring in interior Alaska. Journal of Geophysical Research 101, 12,613–12,619.

Bertman, S.B., Roberts, J.M., Parish, D.D., Buhr, M.P., Goldan, P.D., Kuster, W.C., Fehsenfeld, F.C., Montzka, S.A., Westberg, H., 1995. Evolution of alkyl nitrates with air mass age. Journal of Geophysical Research 100 (D11), 22,805–22,813.

Blake, D., 2004. Methane, nonmethane hydrocarbons, alkyl nitrates, and chlorinated carbon compounds including three chlorofluorocarbons (CFC-11, CFC-12, and CFC-113) in whole-air samples. Trends: A Compendium of Data on Global Change, Carbon Dioxide Information Analysis Center, Oak Ridge National Laboratory, US Department of Energy, Oak Ridge TN, USA.

Blake, N.J., Blake, D.R., Chen, T.-Y., Collins Jr., J.E., Sachse, G.W., Anderson, B.E., Rowland, F.S., 1997. Distribution and seasonality of selected hydrocarbons and halocarbons over the western Pacific basin during PEM-West A and PEM-West B. Journal of Geophysical Research 102 (D23), 28,315–28,331.

Blake, N.J., Blake, D.R., Swanson, A.L., Atlas, E., Flocke, F., Rowland, F.S., 2003a. Latitudinal, vertical, and seasonal variations of C_1–C_4 alkyl nitrates in the troposphere over the Pacific Ocean during PEM-Tropics A and B: oceanic and continental sources. Journal of Geophysical Research 108 (D2).

Blake, N.J., Blake, D.R., Sive, B.C., Katzenstein, A.S., Meinardi, S., Wingenter, O.W., Atlas, E.L., Flocke, F., Ridley, B.A., Rowland, F.S., 2003b. The seasonal evolution of NMHCs and light alkyl nitrates at middle to high northern latitudes during TOPSE. Journal of Geophysical Research 108 (D4).

Buhr, M., Fehsenfeld, F.C., Parrish, D.D., Sievers, R.E., Roberts, J.M., 1990. Contribution of organic nitrates to the total odd-nitrogen budget at a rural, eastern US site. Journal of Geophysical Research 95, 9809–9816.

Chuck, A.L., Turner, S.M., Liss, P.S., 2002. Direct evidence for a marine source of C_1 and C_2 alkyl nitrates. Science 297, 1151–1154.

Clemitshaw, K.C., Williams, J., Rattigan, O.V., Shallcross, D.E., Law, K.S., Cox, R.A., 1997. Gas-phase ultraviolet absorption cross-sections and atmospheric lifetimes of several C_2–C_5 alkyl nitrates. Journal of Photochemistry and Photobiology A: Chemistry 102, 117–126.

Colman, J.J., Swanson, A.L., Meinardi, S., Sive, B.C., Blake, D.R., Rowland, F.S., 2001. Description of the analysis of a wide range of volatile organic compounds in whole air samples collected during PEM-Tropics A and B. Analytical Chemistry 73, 3723–3731.

Darnall, K.R., Carter, W.P.L., Winer, A.M., Lloyd, A.C., Pitts Jr., J.N., 1976. Importance of RO_2+NO in alkyl nitrate formation from C_4–C_6 alkane photooxidations under simulated atmospheric conditions. Journal of Physical Chemistry 80, 1948–1950.

Day, D.A., Dillon, M.B., Wooldridge, P.J., Thornton, J.A., Rosen, R.S., Wood, E.C., Cohen, R.C., 2003. On alkyl nitrates, O_3, and the "missing NO_y". Journal of Geophysical Research 108 (D16), 4501.

DeMore, W.B., Sander, S.P., Golden, D.M., Hampson, R.F., Kurylo, M.J., Howard, C.J., Ravishankara, A.R., Kolb, C.E., Molina, M.J., 1997. Chemical Kinetics and Photochemical Data for Use in Stratospheric Modeling, vol. 12. Publication 97-4, Jet Propulsion Laboratory, California Institute of Technology, Pasadena, CA.

Flocke, F., Volz-Thomas, A., Buers, H.-J., Pätz, W., Garthe, H.-J., Kley, D., 1998a. Long-term measurements of alkyl nitrates in southern Germany. General behavior and seasonal and diurnal variation. Journal of Geophysical Research 103 (D5), 5729–5746.

Flocke, F., Atlas, E., Madronich, S., Schauffler, S.M., Aikin, K., Margitan, J.J., Bui, T.P., 1998b. Observations of methyl nitrate in the lower stratosphere during STRAT: implications for its gas phase production mechanisms. Geophysical Research Letters 25, 1891–1894.

Hofzumahaus, A., Aschmutat, U., Brandenburger, U., Brauers, T., Dorn, H.-P., Hausmann, M., Beßling, M., Holland, F., Plass-Dülmer, C., Sedlacek, M., Weber, M., Ehhalt, D.H., 1998. Intercomparison of tropospheric OH measurements by different laser techniques during the POPCORN campaign, 1994. Journal of Atmospheric Chemistry 31, 227–246.

Karlsdóttir, S., Isaksen, I.S.A., 2000. Changing methane lifetime: possible cause for reduced growth. Geophysical Research Letters 27, 93–96.

Kramp, F., Volz-Thomas, A., 1997. On the budget of OH radicals and ozone in an urban plume from the decay of C_5–C_8 hydrocarbons and NO_x. Journal of Atmospheric Chemistry 28 (1–3), 263–282.

Kwok, E.S.S., Atkinson, R., 1995. Estimation of hydroxyl radical reaction rate constants for gas-phase organic compounds using a structure–reactivity relationship: an update. Atmospheric Environment 29, 1685–1695.

Lelieveld, J., Crutzen, P.J., Dentener, F.J., 1998. Changing concentration, lifetime and climate forcing of atmospheric methane. Tellus 50B, 128–150.

Roberts, J.M., Bertman, S.B., Parrish, D.D., Fehsenfeld, F.C., Jobson, B.T., Niki, H., 1998. Measurement of alkyl nitrates at Chebogue Point, Nova Scotia during the 1993 North Atlantic

Regional Experiment (NARE) intensive. Journal of Geophysical Research 103, 13,569–13,580.

Rosen, R.S., Wood, E.C., Wooldridge, P.J., Thornton, J.A., Day, D.A., Kuster, W., Willliams, E.J., Jobson, B.T., Cohen, R.C., 2004. Observations of total alkyl nitrates during the Texas Air Quality Study 2000: implications for O_3 and alkyl nitrate photochemistry. Journal of Geophysical Research 109, D07303.

Schneider, M., Luxenhofer, O., Deissler, A., Ballschmiter, K., 1998. C_1–C_{15} alkyl nitrates, benzyl nitrate, and bifunctional nitrates: measurements in California and South Atlantic air and global comparison using C_2Cl_4 and $CHBr_3$ as marker molecules. Environmental Science and Technology 32, 3055–3062.

Seinfeld, J.H., Pandis, S.N., 1998. Atmospheric Chemistry and Physics. Wiley, New York.

Shepson, P.B., Anlauf, K.G., Bottenheim, J.W., Wiebe, H.A., Gao, N., Muthuramu, K., Mackay, G.I., 1993. Alkyl nitrates and their contribution to reactive odd nitrogen at a rural site in Ontario. Atmospheric Environment 27A, 749–757.

Simpson, I.J., Meinardi, S., Blake, D.R., Blake, N.J., Rowland, F.S., Atlas, E., Flocke, F., 2002. A biomass burning source of C_1–C_4 alkyl nitrates. Geophysical Research Letters 29 (N24), 2168.

Simpson, I.J., Blake, N.J., Blake, D.R., Atlas, E., Flocke, F., Crawford, J.H., Fuelberg, H.E., Kiley, C.M., Meinardi, S., Rowland, F.S., 2003. Production and evolution of selected C_2–C_5 alkyl nitrates in tropospheric air influenced by Asian outflow. Journal of Geophysical Research 108 (D20), 8808.

Smyth, S., Bradshaw, J., Sandholm, S., Liu, S., McKeen, S., Gregory, G., Anderson, B., Talbot, R., Blake, D., Rowland, S., Browell, E., Fenn, M., Merrill, J., Bachmeier, S., Sachse, G., Collins, J., Thornton, D., Davis, D., Singh, H., 1996. Comparison of free tropospheric western Pacific air mass classification schemes for the PEM-West A experiment. Journal of Geophysical Research 101 (D1), 1743–1762.

Stroud, C.A., Roberts, J.M., Williams, J., Goldan, P.D., Kuster, W.C., Ryerson, T.B., Sueper, D., Parrish, D.D., Trainer, M., Fehsenfeld, F.C., Flocke, F., Schauffler, S.M., Stroud, V.R.F., Atlas, E., 2001. Alkyl nitrate measurements during STERAO 1996 and NARE 1997: intercomparison and survey of results. Journal of Geophysical Research 106 (ND19), 23,043–23,053.

Swanson, A.L., Blake, N.J., Atlas, E., Flocke, F., Blake, D.R., Rowland, F.S., 2003. Seasonal variations of C_2–C_4 nonmethane hydrocarbons and C_1–C_4 alkyl nitrates at the Summit research station in Greenland. Journal of Geophysical Research 108 (D2).

Talbot, R.W., Dibb, J.E., Scheuer, E.M., Bradshaw, J.D., Sandholm, S.T., Singh, H.B., Blake, D.R., Blake, N.J., Atlas, E., Flocke, F., 2000. Tropospheric reactive odd nitrogen over the South Pacific in austral Springtime. Journal of Geophysical Research 105 (D5), 6681–6694.

Talbot, R., Dibb, J., Scheuer, E., Seid, G., Russo, R., Sandholm, S., Tan, D., Singh, H., Blake, D., Blake, N., Atlas, E., Sachse, G., Jordan, C., Avery, M., 2003. Reactive nitrogen in Asian continental outflow over the western Pacific: Results from the NASA TRACE-P airborne mission. Journal of Geophysical Research 108 (D20), 8803.

Talukdar, R.K., Burkholder, J.B., Hunter, M., Gilles, M.K., Roberts, J.M., Ravishankara, A.R., 1997. Atmospheric fate of several alkyl nitrates Part 2 UV absorption cross-sections and photodissociation quantum yields. Journal of the Chemical Society, Faraday Transactions 93 (16), 2797–2805.

Walega, J.G., Ridley, B.A., Madronic, S., Grahek, F.E., Shetter, J.D., Sauvain, T.D., Hahn, C.J., Merrill, J.T., Bodhaine, B.A., Robinson, E., 1992. Observations of peroxyacetyl nitrate, peroxyproprionyl nitrate, methyl nitrate and ozone during the Mauna Loa Observatory Photochemistry Experiment. Journal of Geophysical Research 97, 10,311–10,330.

Wang, T., Kwok, Y.H., 2003. Measurement and analysis of a multiday photochemical smog episode in the Pearl River Delta of China. Journal of Applied Meteorology 42, 404–416.

Wang, T., Poon, C.N., Kwok, Y.H., Li, Y.S., 2003. Characterizing the temporal variability and emission patterns of pollution plumes in the Pearl River Delta of China. Atmospheric Environment 37, 3539–3550.

Wang, T., Guo, H., Blake, D.R., Kwok, Y.H., Simpson, I.J., Li, Y.S., 2005. Measurements of trace gases in the inflow of South China Sea background air and outflow of regional pollution at Tai O, Southern China. Journal of Atmospheric Chemistry 52, 295–317.